Theoretical predictions on the QCD critical point

Joaquín Grefa

June 8th - 13th, 2025

Conference on the Intersections
of Particle and Nuclear Physics

Outline

1. The QCD phase diagram
2. Effective models for QCD
3. Lattice QCD constraints
4. Theory and Experiment
5. Summary

Table of Contents

QCD Phase Diagram

We can explore the QCD phase diagram by changing $\sqrt{s}$ in relativistic heavy ion collisions

Models predict a first order phase transition line with a critical point

Lattice QCD is the most reliable theoretical tool to study the QCD phase diagram.

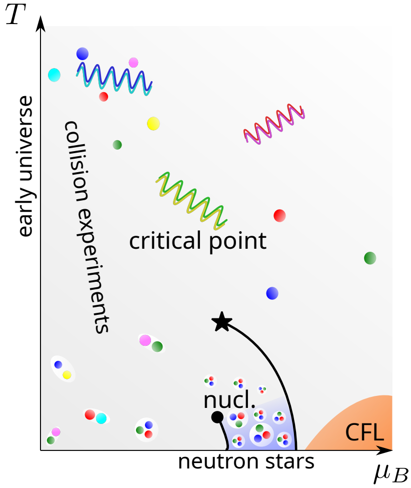

QCD Phase Diagram

We can explore the QCD phase diagram by changing $\sqrt{s}$ in relativistic heavy ion collisions

Models predict a first order phase transition line with a critical point

Lattice QCD is the most reliable theoretical tool to study the QCD phase diagram.

Sign problem:

Equation of state for low to moderate μ_B/T.

Borsányi, Fodor, Guenther et al., PRL **126** (2021)

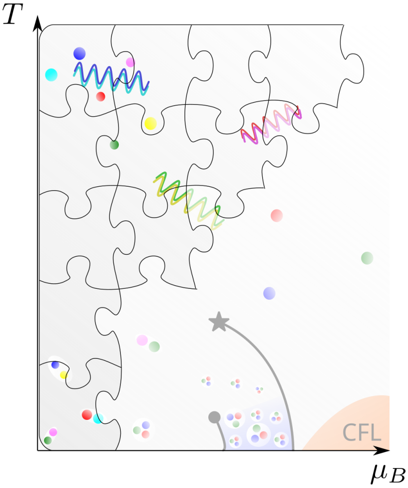

Why a critical point?

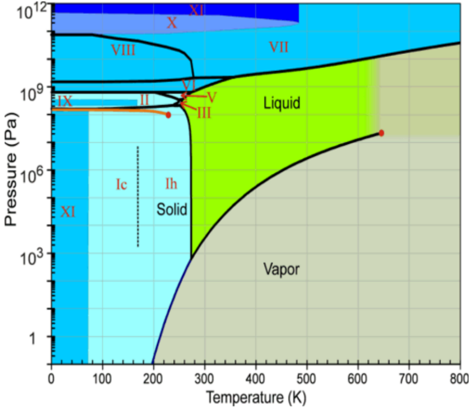

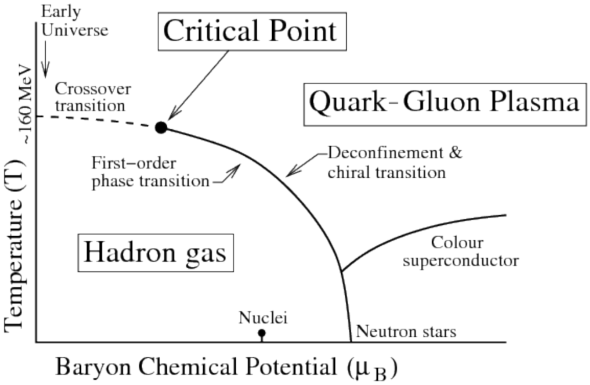

Why a critical point?

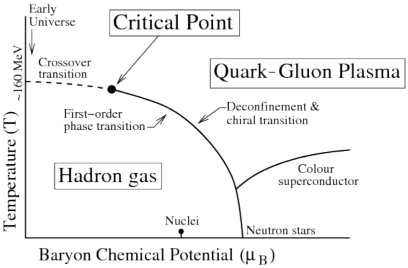

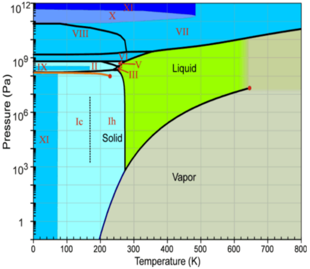

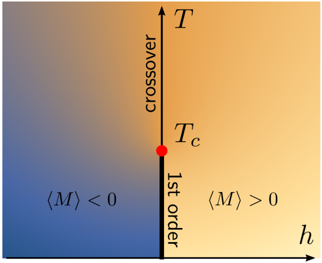

Table of Contents

Model Requirements

We need a simplified theoretical framework that describes QCD in the desired energy range.

Interpret data $\Longleftrightarrow$ make predictions

Requirements:

- QCD symmetries, degrees of freedom, thermodynamics, and/or interactions.
- Agreement with Lattice EoS at $\mu_B = 0$
- Agreement with lattice susceptibilities at $\mu = 0$

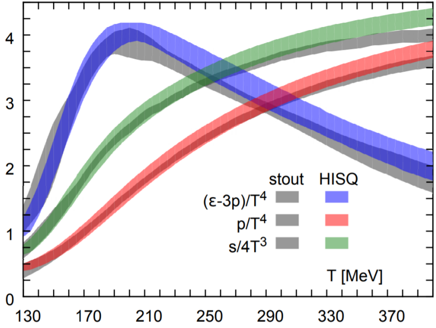

stout: S. Borsanyi et al., 1309.5258, PBL (2014)
HISQ: A. Bazavov et al., 1407.6387, PRD (2014)

Critical point predictions as of some years ago

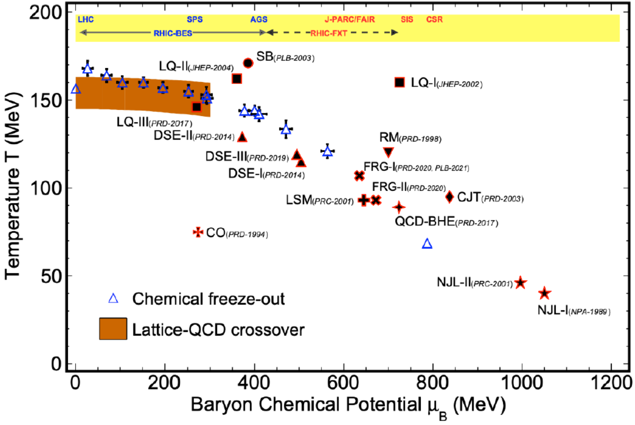

Figure adapted from A. Pandav, D. Mallick, B. Mohanty, Prog. Part. Nucl. Phys. 125 (2022)

- Including the scenario of no critical point at all.
  de Forcrand, Philipsen, JHEP 01, 077 (2007); VV, Steinheimer, Philipsen, Stoecker, PRD 97, 114030 (2018)

Holography (Black Hole engineering - EMD model - gauge/gravity duality)

O DeWolfe et al. Phys.Rev.D 83, (2011). R Rougemont et al. JHEP(2016)102. R. Critelli et al., Phys.Rev.D96(2017).

$$S = \frac{1}{2\kappa_5^2}\int_{M_5} d^5x\sqrt{-g}\left[R - \frac{(\partial_\mu\phi)^2}{2} - \underbrace{V(\phi)}_{\text{nonconformal}} - \underbrace{\frac{f(\phi)F_{\mu\nu}^2}{4}}_{\mu_B\neq 0}\right]$$

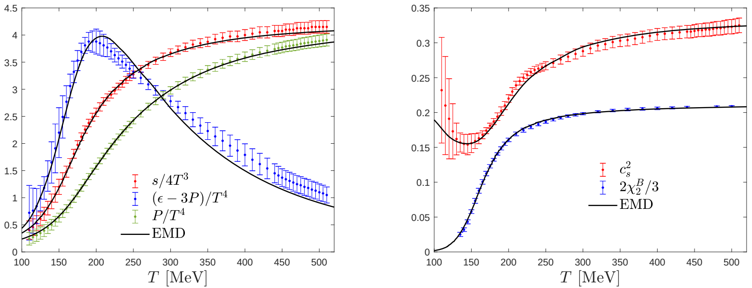

Holographic Bayesian Analysis: posterior critical points

$(T_c,\, \mu_{Bc})_{PHA} = (104 \pm 3,\, 589^{+36}_{-26})$ MeV, $(T_c,\, \mu_{Bc})_{PA} = (107 \pm 1,\, 571 \pm 11)$ MeV.

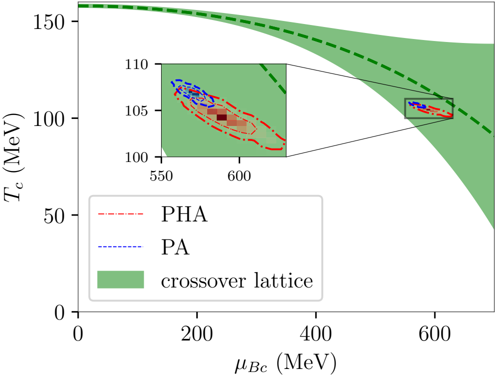

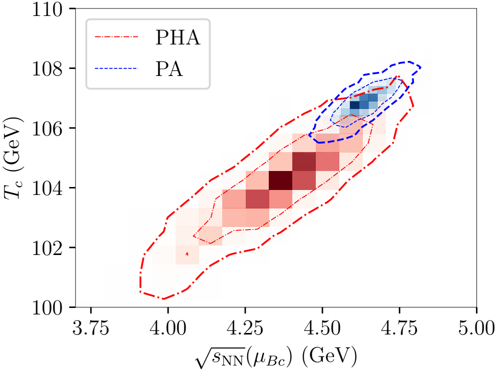

- Both Ansätze overlap at $1\,\sigma$. **Robust results!**

M. Hippert, J.G., T.A. Manning. J. Noronha, J. Noronha-Hostler, I. Portillo, C. Ratti, R. Rougemont, M. Trujillo, arXiv:2309.00579.

Functional methods

Based on the truncated expansion of the QCD functional, and requires control of errors to compute thermodynamics.

Dyson–Schwinger Equations (DSE)

- integral equations derived from the QCD action that relate the propagators (Green's functions) of quarks and gluons to each other.
- are solved approximately using truncation schemes and modeling of the interaction vertices.

Functional renormalization group (FRG)

- describing how the effective QCD action changes as one varies the energy scale.
- allows for a continuous evolution from microscopic physics to macroscopic phenomena, capturing quantum, thermal, and density fluctuations along the way.

Effective QCD theories prediction

- Different effective approaches, all in excellent agreement with lattice QCD at $\mu_B = 0$ (and $\mu_B/T \sim 3.5$), predict the location of the critical point in a similar region.
- If true, reachable in heavy ion collisions at $\sqrt{s_{NN}} \sim 3 - 5$ GeV.

Dyson-Schwinger equations

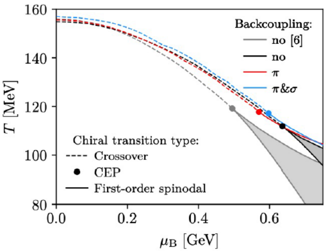

Gunkel, Fischer, PRD 104, 054202 (2021)

Functional renormalization group

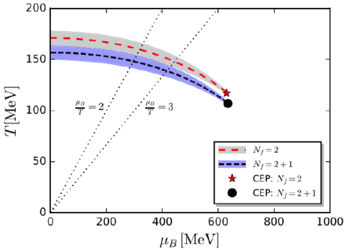

Fu, Pawlowski, Rennecke, PRD 101, 053032 (2020)

Black-hole engineering

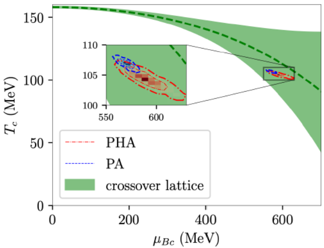

Hippert, J.G., et al., PRD 110, 094006 (2024)

Table of Contents

Entropy density contours

- If lines of constant s cross, it suggests a first order phase transition with a CP; otherwise, the EoS only exhibits a crossover.

$$T_s\left(\mu_B; T_0\right) = T_0 + \alpha_2\left(T_0\right)\frac{\mu_B^2}{2}; \qquad \alpha_2\left(T_0\right) = -\frac{2T_0\chi_2^B(T_0)+T_0^2\chi_2^{B\prime}(T_0)}{s'(T_0)}; \qquad \chi_2^B = \left[\frac{\partial^2(p/T)^4}{\partial(\mu_B/T)^2}\right]_T$$

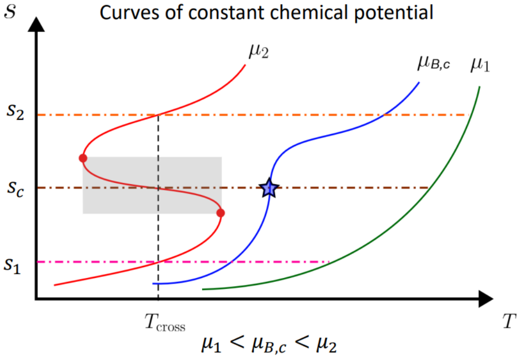

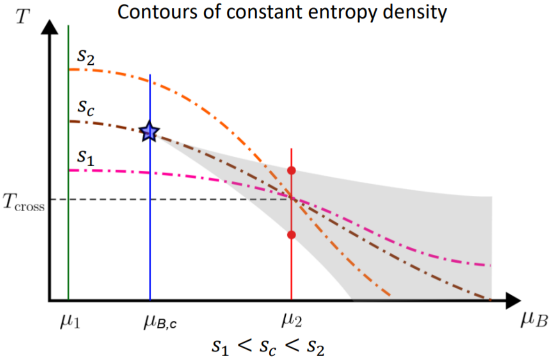

H. Shah et al. arXiv:2410.16026

Entropy density contours

- Excelent agreement with state-of-the-art lattice QCD data up to $\mu_B/T = 3.5$
  Borsanyi et al., PRL 126, 232001 (2021)

$$\mu_B^c = 602 \pm 62 \text{ MeV} \qquad T^c = 114 \pm 7 \text{ MeV}$$

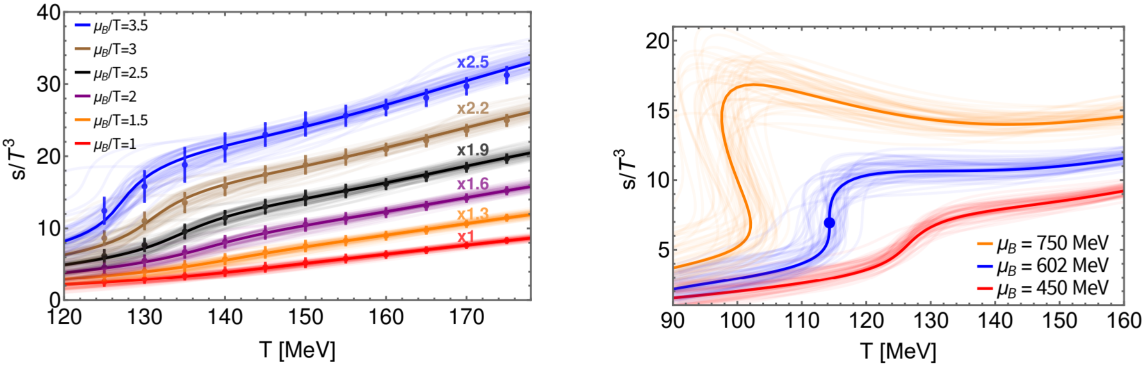

H. Shah et al. arXiv:2410.16026

Constraints with improved lattice data

- New continuum extrapolated equation of state at zero density with improved precision & new data at imaginary chemical potential
- CP excluded at $\mu_B <\sim 450$ MeV

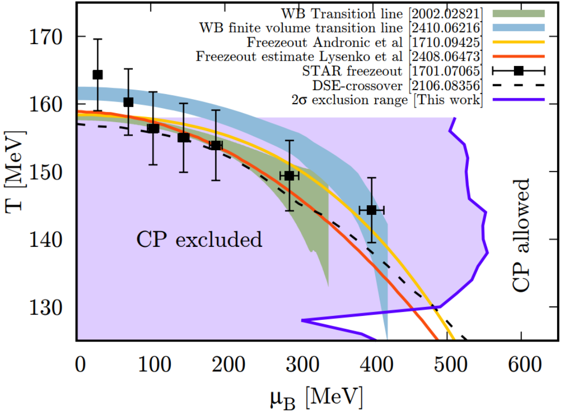

Borsanyi et al. arXiv:2502.1026

Critical point predictions as of some years ago

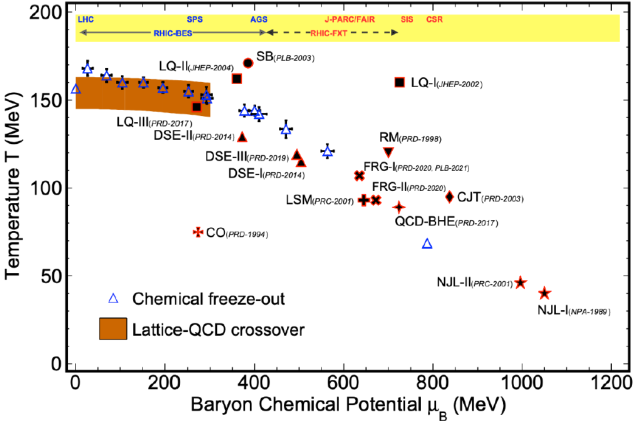

Figure adapted from A. Pandav, D. Mallick, B. Mohanty, Prog. Part. Nucl. Phys. 125 (2022)

- Including the scenario of no critical point at all.
de Forcrand, Philipsen, JHEP 01, 077 (2007); VV, Steinheimer, Philipsen, Stoecker, PRD 97, 114030 (2018)

Critical point with new lattice constraints: no CP at $mu_B < 450$ MeV

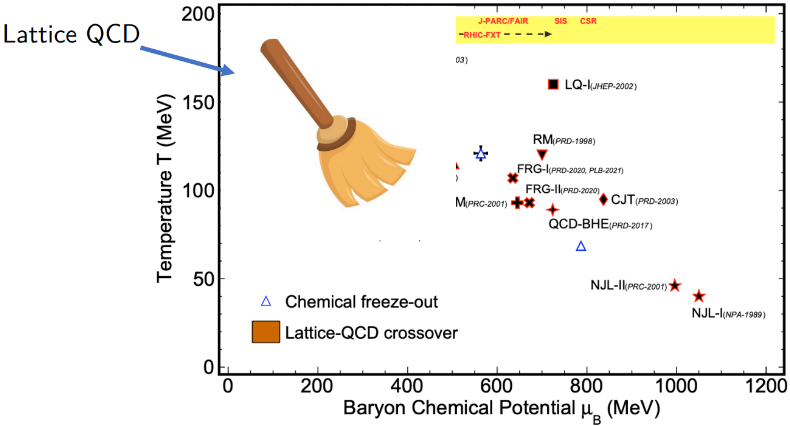

Figure adapted from A. Pandav, D. Mallick, B. Mohanty, Prog. Part. Nucl. Phys. 125 (2022)

- Including the scenario of no critical point at all.
  de Forcrand, Philipsen, JHEP 01, 077 (2007); VV, Steinheimer, Philipsen, Stoecker, PRD 97, 114030 (2018)

Current scenario

- Predictions converge to the same region...

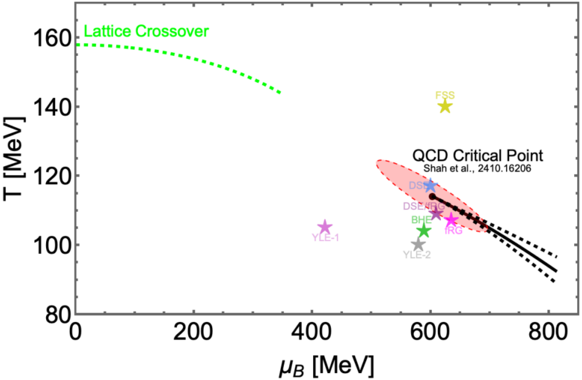

Critical point estimate at $O(\mu_B^2)$:

$T_c = 114 \pm 7$ MeV, $\mu_B = 602 \pm 62$ MeV

Estimates from recent literature:

YLE-1: D.A. Clarke et al. (Bielefeld-Parma), arXiv:2405.10196

YLE-2: G. Basar, PRC 110, 015203 (2024)

BHE: M. Hippert et al., arXiv:2309.00579

fRG: W-J. Fu et al., PRD 101, 054032 (2020)

DSE/fRG: Gao, Pawlowski., PLB 820, 136584 (2021)

DSE: P.J. Gunkel et al., PRD 104, 052022 (2021)

FSS: A. Sorensen et al., arXiv:2405.10278

Adapted from H. Shah et al. arXiv:2410.16026

Current scenario

- Predictions converge to the same region...
  because lattice QCD has not ruled out that region yet?

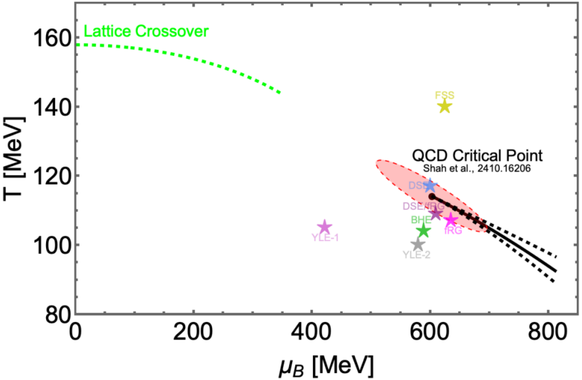

Critical point estimate at $O(\mu_B^2)$:

$T_c = 114 \pm 7$ MeV, $\mu_B = 602 \pm 62$ MeV

Estimates from recent literature:

YLE-1: D.A. Clarke et al. (Bielefeld-Parma), arXiv:2405.10196

YLE-2: G. Basar, PRC 110, 015203 (2024)

BHE: M. Hippert et al., arXiv:2309.00579

fRG: W-J. Fu et al., PRD 101, 054032 (2020)

DSE/fRG: Gao, Pawlowski., PLB 820, 136584 (2021)

DSE: P.J. Gunkel et al., PRD 104, 052022 (2021)

FSS: A. Sorensen et al., arXiv:2405.10278

Adapted from H. Shah et al. arXiv:2410.16026

Table of Contents

Fluctuations

Cumulants measure the chemical potential derivatives of the QCD equation of state

Cumulants as moments of the particle number distribution

variance: $\kappa_2 = \langle (\Delta N)^2 \rangle = \sigma$
skewness: $\kappa_3 = \langle (\Delta N)^3 \rangle$
kurtosis: $\kappa_4 = \langle (\Delta N)^4 \rangle - 3 \langle (\Delta N)^2 \rangle^2$

$$\kappa_2 \sim \xi^2, \quad \kappa_3 \sim \xi^{4.5}, \quad \kappa_4 \sim \xi^7$$

$$\xi \to \infty$$

Cumulants as chemical potential derivatives of the EoS

$$\ln Z(T, V, \mu) = \ln \left[\sum_N e^{\mu N/T} Z^{ce}(T, V, N) \right]$$

$$\kappa_n \propto \frac{\partial^n (\ln Z)}{\partial \mu^n}$$

Critical opalescence

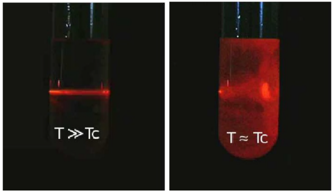

Fluctuations

Cumulants measure the chemical potential derivatives of the QCD equation of state

Cumulants as moments of the particle number distribution

variance: $\kappa_2 = \langle (\Delta N)^2 \rangle = \sigma$
skewness: $\kappa_3 = \langle (\Delta N)^3 \rangle$
kurtosis: $\kappa_4 = \langle (\Delta N)^4 \rangle - 3 \langle (\Delta N)^2 \rangle^2$

$$\kappa_2 \sim \xi^2, \quad \kappa_3 \sim \xi^{4.5}, \quad \kappa_4 \sim \xi^7$$

$$\xi \to \infty$$

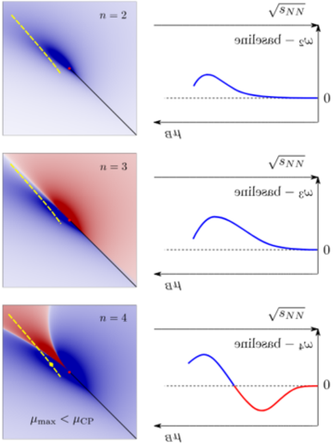

M. Stephanov. SQM 2024

cumulants

- Overall agreement with the baseline for $\sqrt{s_{NN}} \sim 10 - 20$ GeV

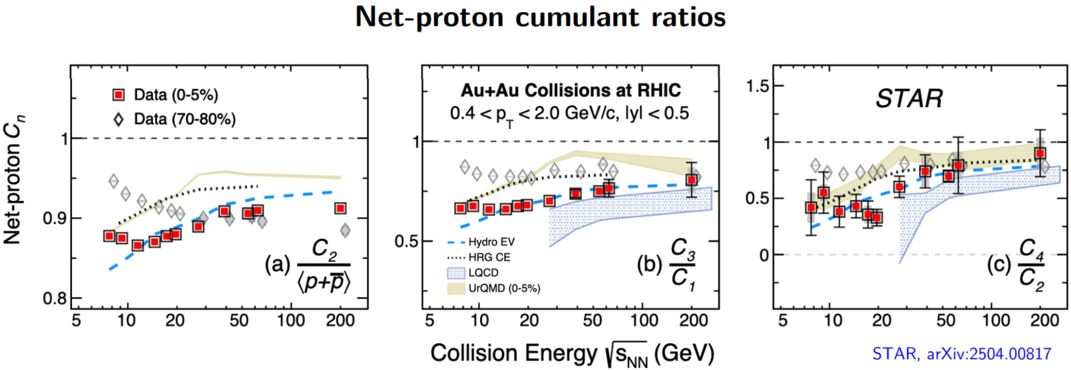

STAR, arXiv:2504.00817

Factorial cumulants!

- Exhibit more structure

Proton factorial cumulant ratios

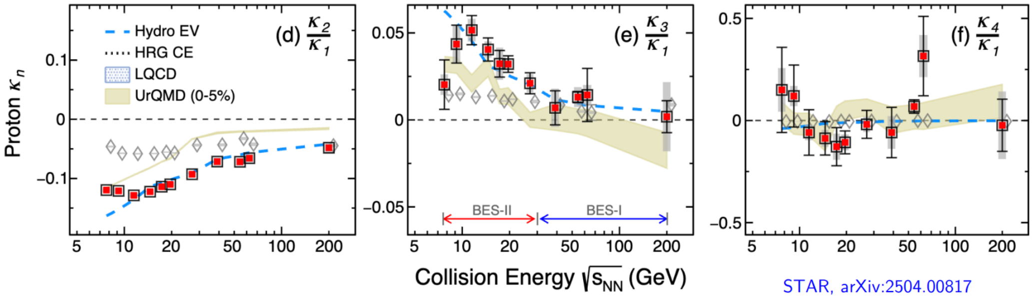

STAR, arXiv:2504.00817

factorial cumulants

V. Vovchenko, arXiv:2504.01368, and adapted from Stephanov, arXiv:2410.02861

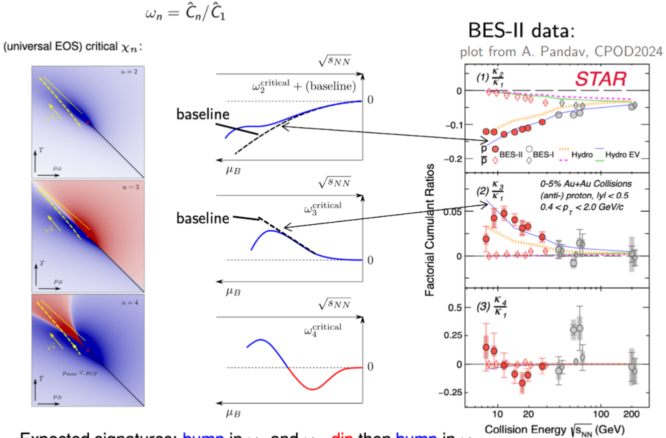

Expected signatures: bump in ω_2 and ω_3, dip then bump in ω_4 for CP at $\mu_B > 420$ MeV

non monotonic κ_2/κ_1, κ_3/κ_1 and maybe κ_4/κ_1

Factorial cumulants: Irreducible n-particle correlations that remove Poisson contribution and probe genuine correlations

Ordinary cumulants: mix correlations of different order

$\hat{C}_n \sim \langle N(N-1)(N-2)\ldots\rangle_c$

$$\hat{C}_1 = C_1$$

$$\hat{C}_2 = C_2 - C_1$$

$$\hat{C}_3 = C_3 - 3C_2 + 2C_1$$

$$\hat{C}_4 = C_4 - 6C_3 + 11C_2 - 6C_1$$

Bzdak, Koch, Strodthoff, PRC 95, 054906 (2017)

Table of Contents

Summary

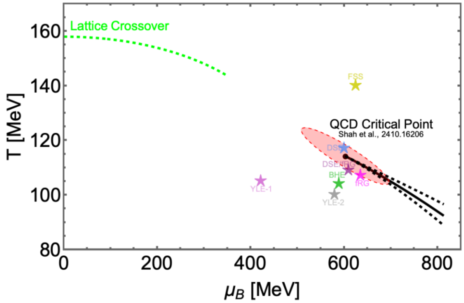

Critical point estimate at $O(\mu_B^2)$:

$T_c = 114 \pm 7$ MeV, $\mu_B = 602 \pm 62$ MeV

Estimates from recent literature:

YLE-1: D.A. Clarke et al. (Bielefeld-Parma), arXiv:2405.10196

YLE-2: G. Basar, PRC 110, 015203 (2024)

BHE: M. Hippert et al., arXiv:2309.00579

fRG: W-J. Fu et al., PRD 101, 054032 (2020)

DSE/fRG: Gao, Pawlowski., PLB 820, 136584 (2021)

DSE: P.J. Gunkel et al., PRD 104, 052022 (2021)

FSS: A. Sorensen et al., arXiv:2405.10278

- No indication of critical behavior from lattice QCD for $\mu_B < 450$ MeV.
- Several effective theories predict the location of the critical point to $T \sim 90 - 120$ MeV and $\mu_B \sim 500 - 650$ MeV.
- No critical behavior describe proton cumulants at $\sqrt{s_{NN}} \geq 20$ GeV.
- This trend changes around $\sqrt{s_{NN}} \sim 10$ GeV; in particular, for factorial cumulants and the presence of the CP could be a reasonable explanation.

Appendix

Ordinary vs. Factorial Cumulants in Heavy-Ion Collisions

Ordinary Cumulants

$C_n \sim \langle \delta N^n \rangle$

- Built from moments of distribution (mean, variance, etc).
- Sensitive to critical fluctuations.
- Connected to thermodynamic susceptibilities.
- Higher orders diverge near critical point.

Factorial Cumulants

$\hat{C}_n \sim \langle N(N-1)(N-2)\ldots \rangle_c$

- Built from factorial moments.
- Vanish for Poisson baseline $\Rightarrow$ better contrast.
- More robust under detection inefficiencies.
- Useful in experimental fluctuation analyses.

Which Cumulants Are Better for the QCD Critical Point?

Both are useful, but serve different purposes:

- **Ordinary cumulants:** $C_n \sim \langle \delta N^n \rangle$
  - Theoretically well-defined.
  - Connected to QCD susceptibilities.
- **Factorial cumulants:** $\hat{C}_n \sim \langle N(N-1)(N-2)\ldots \rangle_c$
  - Cleaner signals under real-world detector conditions.
  - Efficient background suppression (e.g., Poisson noise).
- *Best approach: use both and compare.*

See: Bzdak et al. Phys. Rept. 853 (2020), Kitazawa Asakawa PRC 85 (2012), STAR Collaboration (2022)

What happens at finite/large densities?

- We need to merge the lattice QCD EoS with other effective theories.
- Study the regime of validity of each effective model.
- Constrained internal parameters to adhere know experimental and theoretical limits.
- Test models to validate/exclude them.
- EoS to guide/interpret experimental data.

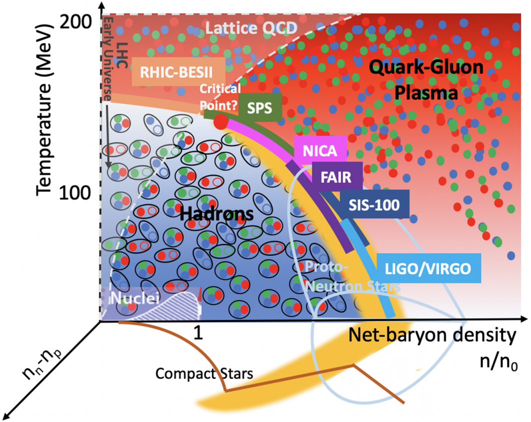

BQS EoS

$10 < T < 600$ MeV; $\mu_B < 450$ MeV

J. Noronha-Hostler, et al., PRC (2019)

$$\frac{p(T,\mu_B,\mu_Q,\mu_S)}{T^4} = \sum_{i,j,k} \frac{1}{i!j!k!} \chi^{BQS}_{ijk} \left(\frac{\mu_B}{T}\right)^i \left(\frac{\mu_Q}{T}\right)^j \left(\frac{\mu_S}{T}\right)^k$$

$$\chi^{BQS}_{ijk} = \left. \frac{\partial^{i+j+k}(p/T^4)}{\partial\left(\frac{\mu_B}{T}\right)^i \partial\left(\frac{\mu_Q}{T}\right)^j \partial\left(\frac{\mu_S}{T}\right)^k} \right|_{\mu_B,\mu_Q,\mu_S=0}$$

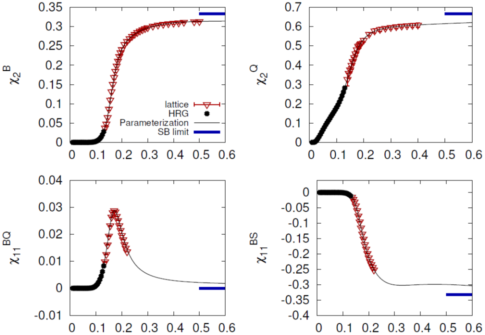

2D Ising T.Ex.S

$10 < T < 800$ MeV; $\mu_B < 700$ MeV

M. Kahangirwe, et al., PRD 109 (2024)

$$T \frac{\chi_1^B(T,\mu_B)}{\mu_B} = \chi_2^B(T',0)$$

$$T'(T,\mu_B) = T\left[1 + \kappa_2^{BB}(T)\left(\frac{\mu_B}{T}\right)^2 + \kappa_4^{BB}(T)\left(\frac{\mu_B}{T}\right)^4 + \dots\right]$$

- Includes a 3D Ising model critical behavior into a lattice alternative expansion EoS.

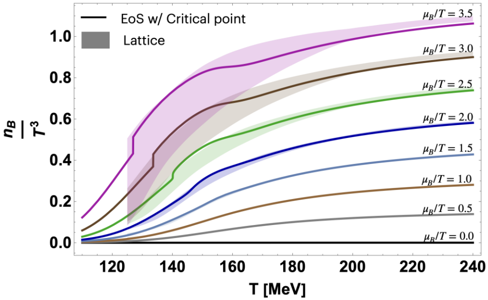

HRG Model

$0 < T < 160$ MeV; $\mu_B < 1000$ MeV

V. Vovchenko, CPC (2019)

- Provides a realistic hadronic EoS at low T
- Interacting hadrons can be modeled by an ideal gas of resonances.
- For a realistic EoS at higher densities, Van der Waals interactions are added.
- Describes the liquid-gas phase transition.

Holography (NumRelHolo)

$40 < T < 400$ MeV; $\mu_B < 1200$ MeV

J. G., et al., PRD (2021), PRD (2022)

- Based on the gauge/gravity duality and constrained to reproduce lattice-QCD thermodynamics
- Large coverage of the EoS in the strongly-interacting regime.
- Predicts the location of the QCD CP.